Publisher's PDF, also known as Version of record

License (if available):
CC BY-NC

Link to published version (if available):
10.1093/brain/awab431

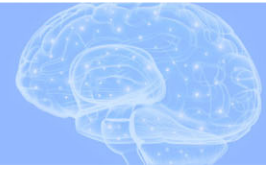Link to publication record in Explore Bristol Research
PDF-document

University of Bristol - Explore Bristol Research
General rights

BRAIN
ORIGINAL ARTICLE

Diagnostic value of cerebrospinal fluid alpha-synuclein seed quantification in synucleinopathies

Ilaria Poggiolini,[1,†] Vandana Gupta,[1,†] Michael Lawton,[2] Seoyun Lee,[1] Aadil El-Turabi,[3] Agustin Querejeta-Coma,[1] Claudia Trenkwalder,[4,5] Friederike Sixel-Döring,[5,6] Alexandra Foubert-Samier,[7,8] Anne Pavy-Le Traon,[9] Giuseppe Plazzi,[10,11] Francesco Biscarini,[12] Jacques Montplaisir,[13,14] Jean-François Gagnon,[13,15] Ronald B. Postuma,[13,16] Elena Antelmi,[17] Wassilios G. Meissner,[8,18] Brit Mollenhauer,[4,5] Yoav Ben-Shlomo,[2] Michele T. Hu[1] and Laura Parkkinen[1]

†These authors contributed equally to this work.

Several studies have confirmed the α-synuclein real-time quaking-induced conversion (RT-QuIC) assay to have high sensitivity and specificity for Parkinson's disease. However, whether the assay can be used as a robust, quantitative measure to monitor disease progression, stratify different synucleinopathies and predict disease conversion in patients with idiopathic REM sleep behaviour disorder remains undetermined. The aim of this study was to assess the diagnostic value of CSF α-synuclein RT-QuIC quantitative parameters in regard to disease progression, stratification and conversion in synucleinopathies.

We performed α-synuclein RT-QuIC in the CSF samples from 74 Parkinson's disease, 24 multiple system atrophy and 45 idiopathic REM sleep behaviour disorder patients alongside 55 healthy controls, analysing quantitative assay parameters in relation to clinical data.

α-Synuclein RT-QuIC showed 89% sensitivity and 96% specificity for Parkinson's disease. There was no correlation between RT-QuIC quantitative parameters and Parkinson's disease clinical scores (e.g. Unified Parkinson's Disease Rating Scale motor), but RT-QuIC positivity and some quantitative parameters (e.g. V_{max}) differed across the different phenotype clusters. RT-QuIC parameters also added value alongside standard clinical data in diagnosing Parkinson's disease. The sensitivity in multiple system atrophy was 75%, and CSF samples showed longer T_{50} and lower V_{max} compared to Parkinson's disease. All RT-QuIC parameters correlated with worse clinical progression of multiple system atrophy (e.g. change in Unified Multiple System Atrophy Rating Scale). The overall sensitivity in idiopathic REM sleep behaviour disorder was 64%. In three of the four longitudinally followed idiopathic REM sleep behaviour disorder cohorts, we found around 90% sensitivity, but in one sample (DeNoPa) diagnosing idiopathic REM sleep behaviour disorder earlier from the community cases, this was much lower at 39%. During follow-up, 14 of 45 (31%) idiopathic REM sleep behaviour disorder patients converted to synucleinopathy with 9/14 (64%) of convertors showing baseline RT-QuIC positivity.

In summary, our results showed that α-synuclein RT-QuIC adds value in diagnosing Parkinson's disease and may provide a way to distinguish variations within Parkinson's disease phenotype. However, the quantitative parameters did not correlate with disease severity in Parkinson's disease. The assay distinguished multiple system atrophy patients from Parkinson's disease patients and in contrast to Parkinson's disease, the quantitative parameters

correlated with disease progression of multiple system atrophy. Our results also provided further evidence for α-synuclein RT-QuIC having potential as an early biomarker detecting synucleinopathy in idiopathic REM sleep behaviour disorder patients prior to conversion. Further analysis of longitudinally followed idiopathic REM sleep behaviour disorder patients is needed to better understand the relationship between α-synuclein RT-QuIC signature and the progression from prodromal to different synucleinopathies.

1   Nuffield Department of Clinical Neurosciences, Oxford Parkinson's Disease Centre, University of Oxford, UK
2   School of Social and Community Medicine, Bristol Medical School, University of Bristol, UK
3   The Jenner Institute, Nuffield Department of Medicine, University of Oxford, UK
4   Department of Neurosurgery, University Medical Center Goettingen, Göttingen, Germany
5   Paracelsus Elena Klinik, Centre for Movement Disorders, Kassel, Germany
6   Department of Neurology, Philipps-University Marburg, Germany
7   French Reference Centre for MSA, University Hospital Bordeaux, Bordeaux, France
8   Institute des Maladies Neurodégénératives, CHU Bordeaux and Univ. Bordeaux, CNRS, IMN, UMR 5293, Bordeaux, France
9   French Reference Centre for MSA, University Hospital of Toulouse, Toulouse, France
10 Department of Biomedical, Metabolic and Neural Sciences, University of Modena and Reggio Emilia, Modena, Italy
11 IRCCS—Institute of the Neurological Sciences of Bologna, Bologna, Italy
12 Department of Biomedical and Neuromotor Sciences (DIBINEM), University of Bologna, Bologna, Italy
13 Center for Advanced Research in Sleep Medicine, CIUSSS-NÎM-Hôpital du Sacré-Cœur de Montréal, Montreal, Quebec, Canada
14 Department of Psychiatry, Université de Montréal, Montreal, Quebec, Canada
15 Department of Psychology, Université du Québec à Montréal, Montreal, Quebec, Canada
16 Department of Neurology, McGill University, Montreal General Hospital, Montreal, Quebec, Canada
17 Department of Neurosciences, Biomedicine and Movement Sciences, University of Verona, Verona, Italy
18 Department of Medicine, University of Otago, Christchurch, and New Zealand Brain Research Institute, Christchurch, New Zealand

Correspondence to: Laura Parkkinen
Nuffield Department of Clinical Neurosciences, University of Oxford
John Radcliffe Hospital, West wing, Level 6, Oxford, OX3 9DU, UK
E-mail: laura.parkkinen@ndcn.ox.ac.uk

Introduction

Synucleinopathies, such as Parkinson's disease, dementia with Lewy bodies and multiple system atrophy (MSA), are defined by aggregation of α-synuclein (αSyn) in neurons and glia but show distinct clinical and pathological features. Parkinson's disease has a long, prodromal phase followed by motor symptoms and at later stages dementia in the majority of patients.[1,2] Cognitive deficits appear earlier and progress faster in dementia with Lewy bodies than in Parkinson's disease,[3] but these two diseases cannot be distinguished pathologically. MSA is characterized by a variable combination of parkinsonism, cerebellar ataxia and autonomic dysfunction and has distinctive pathology, as αSyn aggregation predominantly occurs in oligodendrocytes rather than neurons as in Parkinson's disease and dementia with Lewy bodies.[4] The symptoms of Parkinson's disease, dementia with Lewy bodies and MSA can resemble one another and early clinical diagnosis is difficult, leading to misdiagnosis in up to 40% of cases.[5,6] Idiopathic REM sleep behaviour disorder (iRBD) is by far the strongest clinical prodromal marker for synucleinopathy. Long-term follow-up studies have shown that patients with iRBD patients will eventually develop Parkinson's disease, dementia with Lewy bodies or less commonly MSA.[7–10] The recent multicentre international iRBD study showed the overall conversion rate was 6.3% per year, with 73.5% converting after 12-year follow-up.[11] Accurate identification of iRBD patients at highest risk of imminent phenoconversion would facilitate recruitment into clinical trials aimed at delaying or preventing the onset of synucleinopathies.

Under the disease condition, misfolded and aggregated αSyn recruits endogenous αSyn to aggregate, and this self-perpetuating process spreads throughout the brain-periphery axis.[12–14] This observation may provide a molecular explanation for disease progression also in humans. The phenotypic and pathological diversity of synucleinopathies is hypothesized to be associated with specific αSyn strains, analogous to prion diseases. Although the classification of the αSyn 'strains' is yet to be better determined, many recent studies have attempted to describe them through biochemical, pathological and structural characterization.[15–20] Importantly, αSyn aggregation is not limited to the brain but is also found in biofluids, e.g. CSF,[21] and peripheral tissues, e.g. gut,[22,23] olfactory mucosa[24] and skin.[25] Thus, detecting αSyn aggregation in such accessible media may be a compelling biomarker, especially as the disease process starts years before the onset of clinical symptoms.

We were first to adapt the highly specific and sensitive real-time quaking induced conversion (RT-QuIC) assay to detect αSyn aggregation in the CSF of patients with pathologically confirmed Parkinson's disease and dementia with Lewy bodies.[26] Interestingly, a few analysed cases with iRBD also showed a positive signal, suggesting that our assay had potential as an early diagnostic test for prodromal disease. Since then, several other groups have confirmed the high sensitivity and specificity for synucleinopathies with seeding aggregation assays.[27–30] In RT-QuIC, the reaction is initiated by the biological sample (seed), where the pathological αSyn aggregates induce the aggregation of the recombinant (rec) αSyn (substrate). The kinetics of αSyn aggregation are monitored in real-time by the fluorescence of thioflavin T (ThT), a dye that associates with amyloid-β structures of the aggregating αSyn. The assay delivers a yes/no answer in regard to αSyn polymerization with high sensitivity and specificity. However, we do not know yet whether RT-QuIC could also deliver reproducible and robust quantitative data to stratify between different synucleinopathies and measure disease severity and progression. Here, we used well-characterized longitudinal cohorts of Parkinson's disease and MSA patients to examine whether RT-QuIC quantitative data distinguish between Parkinson's disease and MSA and correlate with clinical symptoms. Finally, we pool four different iRBD cohorts to determine whether RT-QuIC can detect those at imminent risk of phenoconversion to synucleinopathy, thus improving prodromal stratification.

Materials and methods

CSF samples

We analysed 74 Parkinson's disease patients and 17 healthy controls from the Discovery cohort of the Oxford Parkinson's Disease Centre, one of the world's top 10 leading Parkinson's disease biomarker cohorts.[31] To increase the number of healthy controls, we analysed *in vivo* CSF from 32 post-mortem verified controls with no pathological changes from the OPTIMA cohort (Oxford Project to Investigate Memory and Ageing).[26] We also examined CSF samples from 24 MSA patients, 23 from the longitudinal cohort from the French Reference Centre for MSA and one Discovery Parkinson's disease patient rediagnosed as MSA during clinical follow-up. Fifteen (63%) were diagnosed with the MSA parkinsonian type (MSA-P) and nine (37%) the MSA cerebellar type (MSA-C) clinical phenotype.[4] Finally, CSF samples were analysed from a total of 45 polysomnographically verified iRBD patients pooled from four different cohorts: (i) *De Novo* Parkinson (DeNoPa) from the Paracelsus-Elena-Klinik, Kassel, Germany, where 18 iRBD patients and 26 baseline/longitudinal samples were available; (ii) IRCCS—Institute of the Neurological Sciences of Bologna, Italy (11 iRBD

patients, only baseline samples); (iii) Center for Advanced Research in Sleep Medicine, Montreal, Canada (10 iRBD patients, only baseline samples); and (iv) Discovery cohort (six iRBD patients, only baseline samples). From the Montreal cohort, we also analysed six controls (totalling 55 controls with the Discovery and OPTIMA cohorts). CSF was collected and processed as described in all the cohorts[32,33] and stored at –80°C within 30 min of collection. CSF haemoglobin was analysed as described[34] and samples with haemoglobin levels >200 ng/ml were excluded from the analysis. αSyn was quantitated by enzyme-linked immunosorbent assay (ELISA; BioLegend) and phospho-tau/amyloid-β 1–42 using a highly standardized microbead-based immunoassay (Alz Bio3 kit, Fujirebio).

Clinical diagnosis and assessment

The demographics of different study cohorts are shown in Table 1. The study was approved by the local ethics committees and all participants provided written informed consent according to the Declaration of Helsinki. The Discovery Parkinson's disease patients were diagnosed using UK Parkinson's Disease Brain Bank criteria, following specialist neurologist review. The diagnosis of Discovery iRBD patients was made based on polysomnographic evidence according to the International Classification of Sleep Disorders criteria, third edition (ICSD3). The Discovery Parkinson's disease and iRBD patients underwent in-depth phenotyping at 18-month intervals, including clinical scores assessing motor, non-motor and cognitive domains fully described elsewhere.[7,35,36] Clinical assessments included motor assessments, e.g. Movement Disorders Society Unified Parkinson's disease Rating Scale (MDS-UPDRS) parts I to IV and cognitive assessments, e.g. Mini-Mental State Examination (MMSE) and Montreal Cognitive Assessment (MoCA). The Discovery Parkinson's disease patients were further divided into four clusters according to the previously published data-driven approach: (i) fast motor progression with symmetrical motor disease, poor olfaction, cognition and postural hypotension; (ii) mild motor and non-motor disease with intermediate motor progression; (iii) severe motor disease, poor psychological well-being and poor sleep with an intermediate motor progression; and (iv) slow motor progression with tremor-dominant unilateral disease.[37]

The diagnosis of 'probable' MSA was made according to current consensus criteria.[4] Disease severity was assessed at baseline and follow-up visits with the Unified Multiple System Atrophy Rating Scale (UMSARS). CSF was collected as part of the BIOAMS (NCT01485549) and BIOPARK (NCT02114242) cohort studies.[38]

DeNoPa iRBD patients were diagnosed as extensively detailed elsewhere,[39–42] assessed according to the DeNoPa protocol[32,43] and followed every 24 months. Both Bologna and Montreal iRBD patients were diagnosed according to ICSD3, assessed as described[44,45] and followed biannually and annually, respectively. For all iRBD patients, an array of prodromal markers were collected at each visit including motor and cognitive function, depression and anxiety, special senses (e.g. smell) and autonomic function.

Expression and purification of human recombinant α-synuclein

A single batch (∼10 mg) of full-length human recombinant αSyn (1–140) was purified and used in this study. BL21(DE3)-pRARE2 (Rosetta) *Escherichia coli*-competent cells were transformed with the pET-28b-6H TEV plasmid containing wild-type human αSyn and cultured overnight at 37°C with vigorous shaking at 200 rpm in TB (Terrific) broth medium. When the absorbance reached 0.3–0.5 OD$_{600}$, protein expression was induced with the addition of 50 μM

Table 1 Demographic characteristics in the different patient and control cohorts

	Parkinson's disease (n = 74)	iRBD[a] (n = 45)	Controls (n = 55)	MSA (n = 24)	P-value
Sex, male n (%)	48 (64.9)	33 (73.3)	28 (50.9)	14 (58.3)	0.13
Age at lumbar puncture	65.3 ± 9.0 (39.7–83.6)	65.7 ± 8.4 (46.0–80.0)	76.4 ± 11.9 (51.8–99.0)	63.8 ± 8.2 (47.0–76.0)	<0.001
Duration from diagnosis to lumbar puncture, years	2.1 ± 1.4 (0.2–5.7)	4.9 ± 4.5 (0.2–20.0)		5.7 ± 3.2 (1.0–15.0)	NA
MDS-UPDRS part I	8.9 ± 5.3 (0–25)	11.2 ± 5.0 (2–20)			0.041
MDS-UPDRS part II	9.1 ± 6.2 (1–29)	2.8 ± 3.0 (0–10)			<0.001
MDS-UPDRS part III	26.8 ± 11.8 (7–74)	3.8 ± 3.6 (0–12)	2.5 ± 2.7[a] (0–9)		<0.001
MDS-UPDRS part IV	0.6 ± 2.0 (0–15)				
Hoehn and Yahr stage	2.0 ± 0.4 (1–3)				
MMSE	27.6 ± 2.3 (19–30)	28.5 ± 1.1 (26–30)	29.0 ± 1.1 (26–30)[a]		0.009
MoCA	25.2 ± 3.1 (17–30)	25.9 ± 2.1(21–29)	27.6 ± 1.8 (24–30)[a]		0.001
MSA subtype (MSA-P), n (%)				14 (60.9)	
UMSARS baseline				44.4 ± 17.5 (12–81)	
UMSARS follow-up				55.5 ± 21.3 (23–95)	
UMSARS change[b]				10.2 ± 5.2 (–0.8–22.0)	

Data are mean ± SD (range) unless otherwise stated. P-values evaluated with a chi-square or Kruskal–Wallis test.
[a]OPTIMA cohort not included.
[b]Change from baseline to follow-up divided by number of years between assessments

isopropyl β-ᴅ-1-thiogalactopyranoside for 16 h at 25°C. Cells were then harvested by centrifugation and the pellet was resuspended in lysis buffer [20 mM Tris pH 8, 150 mM NaCl, protease inhibitor cocktail (EDTA-free), 2 mM MgSO$_4$, 0.1% Triton X-100, Benzonase and 0.5 mg/l lysozyme]. The cell suspension was incubated for half an hour on ice. The suspension was sonicated and the lysate was centrifuged at 30 000g for 20 min. Three millilitres of an 80% slurry of nickel beads (GE Healthcare) per litre of cells was added to the supernatant, the mixture was incubated for 1 h in the cold room with gentle end-over-end rotation. Beads were washed with 20 column volumes of binding buffer (20 mM Tris 8.0, 150 mM NaCl, 10 mM imidazole) followed by 20 column volumes of wash buffer (20 mM Tris 8.0, 150 mM NaCl, 20 mM imidazole). αSyn was eluted with elution buffer (20 mM Tris 8.0, 150 mM NaCl, 300 mM imidazole), samples from the eluted peak fractions were pooled together and dialysed into 20 mM Tris 8.0, 2 mM EDTA, 100 mM NaCl overnight at 4°C in the presence of tobacco etch virus (TEV) protease. After digestion, His-tag was separated from the protein through affinity chromatography. The fractions containing the greatest amount of αSyn were pooled, diluted 2.5-fold with IEX-0 buffer (20 mM Tris, 2 mM EDTA, 0 mM NaCl) and loaded onto a 1-ml Q-Sepharose column. The column was then washed with 50 column volumes of IEX-0, followed by 50 column volumes of IEX-25 (20 mM Tris 8.0, 2 mM EDTA, 25 mM NaCl). αSyn was eluted with IEX-300 (20 mM Tris 8.0, 2 mM EDTA, 300 mM NaCl). Fractions containing the protein were pooled together and concentrated before loading onto a size-exclusion column (Sephacryl S-200 HR). Peak fractions were collected (10 mM Tris 7.5, 0.1 M NaCl) and pooled at a concentration of 1 mg/ml. The identity and purity of the final product was confirmed by both SDS Page and mass spectroscopy. The 200-μl aliquots were then prepared and stored at –80°C. Prior to use, the protein was filtered with 100-kDa spin filter (Pall).

RT-QuIC assay

RT-QuIC assay was performed using purified human recombinant αSyn with re-optimized assay conditions as previously described.[26] The reaction buffer was composed of 0.1 M PIPES (pH 7.0), 0.1 mg/ml recombinant αSyn and 10 μM ThT. Reactions were performed in duplicates in a black 96-well plate with a clear bottom (Nunc, Thermo Fischer) with 85 μl of the reaction mix loaded into each well together with 15 μl of neat CSF. The plate was sealed with a sealing film (Thermo Fischer) and incubated in a BMG Labtech FLUOstar OMEGA plate reader at 40°C for 120 h with intermittent cycles of 1 min shaking (500 rpm, double orbital) and 1 min rest throughout the indicated incubation time. The ThT fluorescence measurements, expressed as arbitrary relative fluorescence units (RFU), were taken every 30 min using 450 ± 10 nm (excitation) and 480 ± 10 nm (emission). A positive RT-QuIC signal was defined as RFU > 5 SD above the mean of initial fluorescence at 120 h. If only one of two CSF samples gave a positive response, the RT-QuIC analysis was replicated in quadruplicate. The sample was then considered positive if two or more of the replicates were positive, otherwise the sample was considered negative. All the RT-QuIC examinations were done blindly without any information regarding clinical data. As well as determining if the assay was positive or not, the relative αSyn seeding activity was extrapolated by plotting RFU readouts against assay time as follows (Supplementary Fig. 1): (i) T$_{lag}$ (hours) is defined as the time interval between the beginning of the reaction and the time in which the curve of the fluorescent signal crosses the threshold (RFU > 5 SD); (ii) F$_{max}$ is defined as the maximum ThT fluorescence in the stationary phase; (iii) T$_{50}$ (hours) is defined as the time latency to obtain 50% of the maximum relative fluorescence; (iv) V$_{max}$—maximum slope of the amplification curve—is determined as the maximum increase in relative fluorescence over time; (v) area under the curve (AUC), for a given time interval (t$_1$–t$_2$), can be calculated as follows: AUC = 1/2 (C$_1$ + C$_2$) (t$_2$ – t$_1$). C$_1$ + C$_2$ is the average concentration over time interval.

Statistical analysis

We examined descriptive statistics and transformed continuous RT-QuIC parameters as appropriate. Differences in these parameters across the patient groups were assessed using ANOVA or Kruskal–Wallis tests depending on if the overall model showed evidence the residuals were not normally distributed. We used Spearman rank correlations or Kruskal–Wallis tests to look at the associations between the disease variables and the RT-QuIC parameters. We used linear or logistic regression models with the transformed RT-QuIC positivity or parameters as the outcomes, respectively, adjusting for age, sex and disease duration separately for Parkinson's disease, MSA and iRBD patients. The transformations we used were: square root for F$_{max}$, V$_{max}$, AUC, phospho-tau

Table 2 RT-QuIC parameters and ELISA biomarkers against the patient groups

	PD (n = 74)	iRBD (n = 45)	Controls (n = 55)	MSA (n = 24)	P-value	P-value PD versus RBD	P-value PD versus MSA	P-value RBD versus MSA	ROC (95% CI) PD versus RBD	ROC (95% CI) PD versus MSA	ROC (95% CI) RBD versus MSA
RT-QuIC positive response, n (%)	66 (89.2%)	29 (64.4%)	2 (3.6%)	18 (75%)	<0.001	0.002	0.10	0.43			
T_{lag}, h[a]	66.0±27.1 (24.0–120.0)	81.9±33.3 (32.0–120.0)	116.7±17.3 (20.0–120.0)	70.4±32.7 (30.0–120.0)	<0.001	0.014	0.70	0.22	0.63 (0.53–0.74)	0.53 (0.39–0.67)	0.59 (0.45–0.73)
F_{max}, RFU × 10^5[a]	1.85±0.90 (0.20–2.60)	1.32±1.05 (0.21–2.60)	0.31±0.36 (0.19–2.60)	1.47±1.01 (0.22–2.60)	<0.001	0.012	0.096	0.51	0.63 (0.53–0.74)	0.61 (0.48–0.74)	0.55 (0.41–0.68)
T_{50}, h[a]	77.1±25.4 (36.0–120.0)	90.0±29.7 (33.0–120.0)	116.9±16.4 (27.0–120.0)	92.9±25.0 (43.0–120.0)	<0.001	0.016	0.009	0.80	0.63 (0.52–0.74)	0.68 (0.55–0.80)	0.52 (0.38–0.66)
V_{max} × 10^4[a]	4.86±4.83 (0.15–22.93)	3.57±4.96 (0.15–22.59)	0.71±2.50 (0.15–14.01)	2.42±4.56 (0.14–22.78)	<0.001	0.019	<0.001	0.34	0.63 (0.52–0.74)	0.74 (0.63–0.85)	0.57 (0.43–0.71)
AUC × 10^6[a]	8.27±5.73 (0.14–21.59)	6.38±4.09 (1.21–14.89)	2.96±3.12 (1.90–23.19)	8.66±5.29 (1.96–20.10)	<0.001	0.14	0.53	0.089	0.58 (0.48–0.69)	0.54 (0.41–0.68)	0.63 (0.48–0.77)
ELISA data											
aSyn, pg/ml	617±331 (147–1870)	792±221 (489–1145)	797±418 (265–1664)		0.072	0.11			0.73 (0.57–0.90)		
Aβ 1–42, pg/ml	541±129 (274–889)		626±246 (394–1322)		0.12						
p-tau, pg/ml	41.0±17.3 (10.3–103.6)		62.2±24.9 (10.3–98.5)		<0.001						
p-tau/Aβ 1–42	0.08±0.04 (0.02–0.19)		0.10±0.05 (0.02–0.20)		0.053						

Data are mean ± SD (range) unless otherwise stated. Note that the P-values and ROC come from separate analyses. P-values come chi-square, ANOVA or Kruskal–Wallis tests while the ROC comes from a logistic regression where the patient groups are the outcomes. Aβ = amyloid-β; PD = Parkinson's disease.
[a]Showed evidence the residuals were not normally distributed ($P < 0.05$) so non-parametric models were used for this variable.

and phospho-tau/amyloid-β 1–42; log for αSyn and amyloid-β 1–42; along with the inverse of the square root for T_{lag} and T_{50}. After transformation, residuals were still often not normally distributed which is the reason for displaying non-parametric tests. We also compared the RT-QuIC parameters across our validated Parkinson's disease clusters[37] in the same way as the patient groups. We looked at whether the RT-QuIC parameters could predict motor prognosis for Parkinson's disease patients using multilevel models (baseline = intercept, progression = slope).[46] We calculated the probability of prodromal Parkinson's disease using the MDS research criteria,[47] then looked whether any of the RT-QuIC parameters improved the differentiation of Parkinson's disease versus control using logistic regression. Rates of neurological disease-free survival in iRBD patients were estimated using the Kaplan–Meier method.

Data availability

Data are available upon request to the corresponding author.

Results

RT-QuIC performance across Parkinson's disease and controls

To establish a robust and reproducible αSyn RT-QuIC assay, we first tested the influence of substrate on the RT-QuIC performance. We compared the reactions using two different batches of recombinant αSyn (Supplementary Fig. 2A–C) which did not result in statistically significant differences in any RT-QuIC quantitative parameters (V_{max} $P = 0.47$; T_{50} $P = 0.68$; T_{lag} $P = 0.10$; AUC $P = 0.92$). To determine the reproducibility, the quantitative parameters were compared from two independent RT-QuIC assays (Supplementary Fig. 2D–F). Both assays gave strikingly similar response and did not lead to any statistically significant differences in RT-QuIC quantitative parameters (V_{max} $P = 0.46$; T_{50} $P = 0.33$; T_{lag} $P = 0.10$; AUC $P = 0.64$).

After thoroughly assessing the reliability and accuracy of the test, we then examined the performance of the assay in a well-characterized Parkinson's disease patient cohort from the longitudinal Oxford Discovery study. We found that 66 of 74 Parkinson's disease patients and 2 of 55 controls tested positive for the αSyn-RT-QuIC, corresponding to a sensitivity of 89% (95% CI 80, 96%) and specificity of 96% (95% CI 88, 100%; Table 2). Two controls showed a positive RT-QuIC response; one Discovery control who had normal MDS-UPDRS and olfaction and one Montreal control who also had normal MDS-UPDRS, autonomic, cognition, olfaction and quantitative motor testing, but did have bilateral action tremor. To date, neither of these controls have met criteria for Parkinson's disease or any other neurodegenerative disorder. Eight Parkinson's disease patients with a negative RT-QuIC performed better in olfaction testing than their positive counterparts, but there were no significant differences in motor scores or improvement with medication, measured by the Clinical Global Impression of Change (CGI).

Strong evidence of differences was observed for all RT-QuIC parameters between Parkinson's disease and controls ($P < 0.001$; Table 2 and Fig. 1A–E). There were 10 Parkinson's disease patients who had particularly a high V_{max} value of >100 000 RFU/h (Fig. 1D). They were significantly older ($P = 0.03$) and had higher scores in the postural instability gait disorder part of the MDS-UPDRS ($P = 0.05$), whereas no significant differences were found in cognition, Hoehn and Yahr stage, MDS-UPDRS III, tremor subscore or CGI. The log odds of the prodromal Parkinson's disease score strongly associated with Parkinson's disease/control status with an odds ratio of 3.6 (95% CI 2.0–6.6, $P < 0.001$). However, the addition of each of the RT-QuIC parameters added predictive power with the strongest predictor being positivity as well as the F_{max}
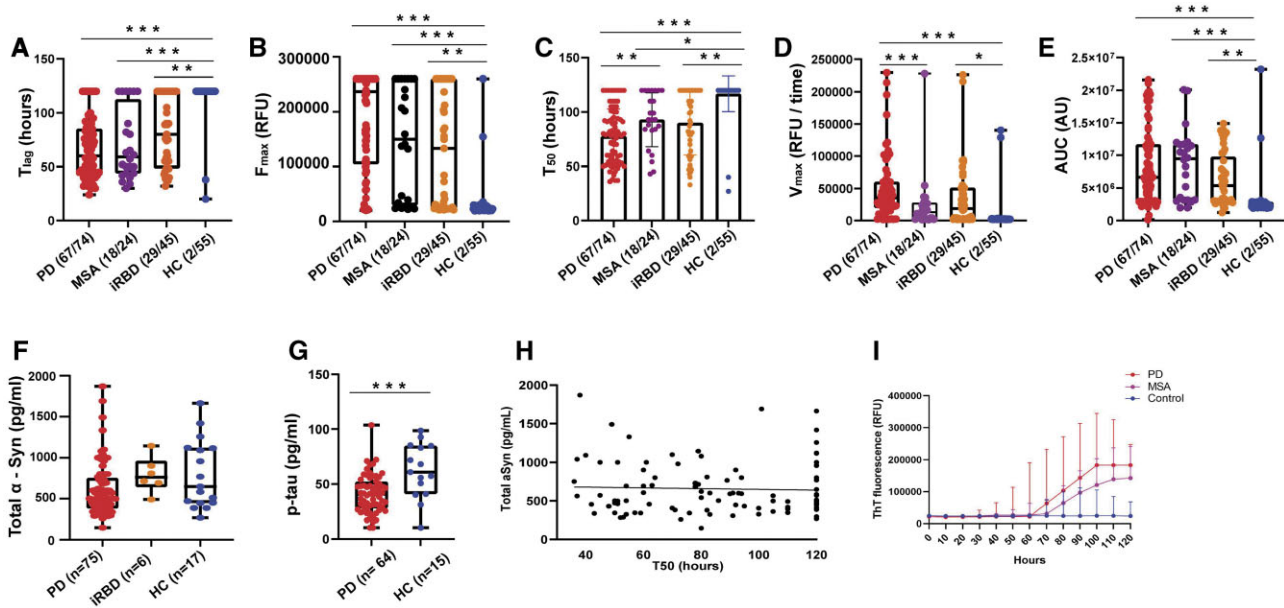
Figure 1 RT-QuIC parameters and other CSF biomarkers in different patient cohorts. (A) The lag phase (T_{lag}) = time each positive reaction exceeds the threshold (RFU > 5 SD); **(B)** the maximum fluorescence value (F_{max}) = highest mean fluorescence value achieved; **(C)** T_{50} = time latency to reach 50% of the F_{max}; **(D)** the maximum slope (V_{max}) = maximum increase per unit of time; and **(E)** the area under curve (AUC). Bars show the average ± SD. **(F)** Levels of total αSyn and **(G)** phospho-tau in the Discovery cohort. Bars show the average ± SD. **(H)** No correlation detected between total αSyn levels and T_{50} values in the Discovery cohort including all Parkinson's disease, iRBD and heathy controls (same cases showed in **G**). **(I)** Kinetic curves of αSyn seeding activity measured by RT-QuIC in Parkinson's disease (red line, *n* = 74) and MSA (purple line, *n* = 24) clinical cases. Each curve depicts the average percentage of ThT fluorescence from duplicate reactions of each group. Each dot depicts average RFU value at 10-h interval. Vertical bars represent the mean ± SD.

Table 3 Associations when added to a logistic regression of Parkinson's disease versus control with the MDS prodromal Parkinson's disease score

	Odds ratio (95% CI)	P-value
RT-QuIC response	85.5 (3.8, 1925.0)	0.005[**]
T_{lag}, h	3.1 (1.2, 8.3)	0.023[*]
F_{max}, RFU	11.9 (2.0, 71.0)	0.006[**]
T_{50}, h	2.4 (1.0, 5.9)	0.051
V_{max}	4.7 (1.4, 15.9)	0.012[*]
AUC	4.8 (1.4, 15.9)	0.011[*]
ELISA data		
aSyn, pg/ml	0.38 (0.12, 1.2)	0.11
Amyloid-β 1–42, pg/ml	0.97 (0.36, 2.6)	0.95
p-tau, pg/ml	0.18 (0.04, 0.84)	0.029[*]
p-tau/Amyloid-β 1–42	0.14 (0.03, 0.69)	0.016[*]

Note that T_{lag} and T_{50} were inverted to normalize the distribution. OPTIMA controls were not included in this analysis as they did not have adequate clinical data to calculate the prodromal risk score.
[*]$P < 0.05$; [**]$P < 0.01$.

value (Table 3). No statistical difference was detected in αSyn (Fig. 1F) or amyloid-β 1–42 CSF concentrations between Parkinson's disease and controls (Table 2). However, phospho-tau levels were significantly lower in Parkinson's disease patients compared to controls ($P < 0.001$; Table 2 and Fig. 1G). We could not detect any relationship between RT-QuIC quantitative parameters and αSyn (e.g. T_{50} Fig. 1H), amyloid-β 1–42 or phospho-tau levels.

Correlation of RT-QuIC parameters with Parkinson's disease severity and clusters

At baseline, there was some evidence that MDS-UPDRS I ($P = 0.003$) and MoCA ($P = 0.04$) were associated with T_{50}, but this was not in

the expected direction (i.e. shorter T_{50} with more severe phenotype; Supplementary Table 1). There was weak evidence that worse MDS-UPDRS IV scores were associated with higher V_{max} values ($P = 0.05$), but this was attenuated after adjustment for age, disease duration and sex (Supplementary Table 2). Adjusted sensitivity analysis also showed MoCA and MMSE strongly associated with T_{50}, but this was not in the expected direction (as above). We found some evidence that being male was related to lower F_{max} ($P = 0.022$), although this was attenuated after adjustment. Analysing RT-QuIC parameters against motor progression (Supplementary Table 3), no parameters were strongly associated with baseline or rate of change in the MDS-UPDRS III except for V_{max}, but this was consistent with chance after adjusting for age and sex. The RT-QuIC parameters differed by Parkinson's disease clusters (Fig. 2 and Supplementary Table 4). Cluster 2 with mild motor and non-motor disease showed the lowest proportion of RT-QuIC responders, whereas all cluster 1 patients with fast motor progression, symmetrical motor disease, poor olfaction, cognition and postural hypotension were RT-QuIC-positive. There was also evidence that V_{max} was different across the clusters ($P = 0.02$), with clusters 1 and 4 having higher V_{max} than clusters 2 and 3.

RT-QuIC performance in multiple system atrophy, stratification from Parkinson's disease and correlation to disease progression

We found 18 of 24 MSA patients tested positive for the αSyn-RT-QuIC (sensitivity 75%, 95% CI 53, 90%). All nine MSA-C patients were RT-QuIC-positive (100%, 95% CI 66, 100%) while only 8 of 14 (57%, 95% CI 29, 82%) MSA-P patients were positive ($P = 0.05$; Table 4). However, there were no significant differences in any of the RT-QuIC parameters between MSA-P and MSA-C subtypes. The average T_{50} was 93 h, and this was significantly higher in MSA compared to Parkinson's disease patients ($P = 0.009$; Table 2 and
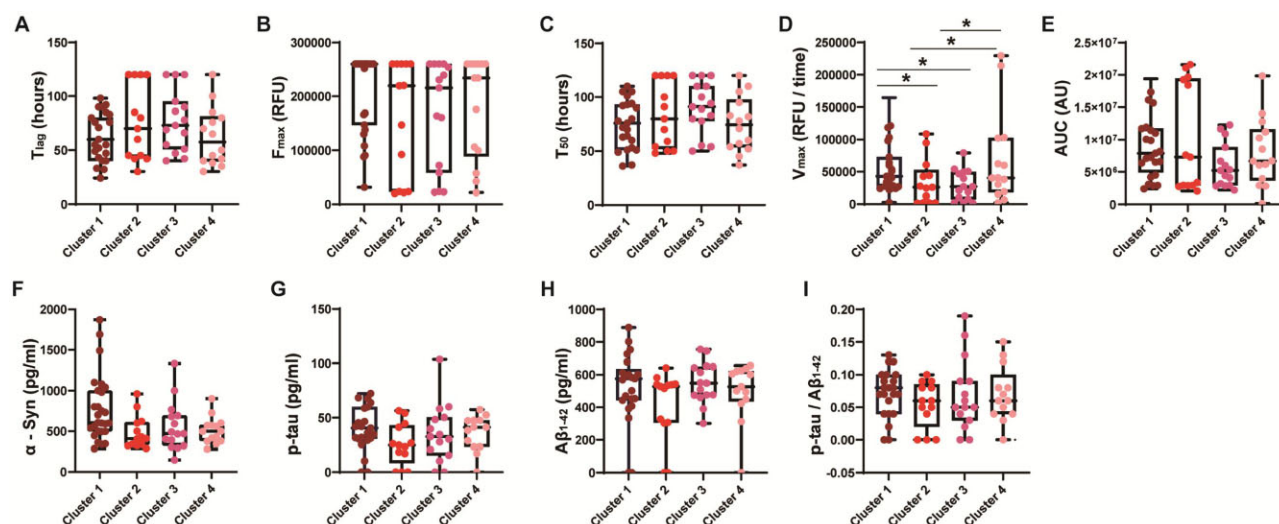
Figure 2 RT-QuIC parameters (A–E) and ELISA biomarkers (F–I) in the Discovery cohort against validated Parkinson's disease clinical clusters. Data are mean ± SD (range) unless otherwise stated. No other changes were detected except (D) V_{max} was different across the clusters ($P = 0.02$), with cluster 1 having higher V_{max} than clusters 2 ($P = 0.02$) and 3 ($P = 0.03$) and cluster 4 having higher V_{max} than clusters 2 and 3 ($P = 0.05$).

Fig. 1C). Only the Discovery MSA patient (initially misdiagnosed as Parkinson's disease) reached the high V_{max} value of $>100\,000$ RFU/h and V_{max} was much lower in the MSA compared to Parkinson's disease patients ($P < 0.001$; Fig. 1D). Receiver operating characteristics curves showed moderate ability of both T_{50} (AUC 0.68 with 95% CI 0.55–0.80) and V_{max} (0.74, 0.63–0.85) to classify a given case as Parkinson's disease or MSA. Correlating the RT-QuIC and disease parameters (Table 4), we found strong evidence that all RT-QuIC parameters were associated with change in the UMSARS from baseline to follow-up, which remained after adjusting for age, sex, disease duration and MSA subtype with the exception of T_{50} (Supplementary Table 5).

RT-QuIC performance and clinical conversion in the idiopathic REM sleep behaviour disorder cohorts

We found 29 of 45 iRBD patients to be positive at baseline (64% sensitivity, 95% CI 49, 78%) and 35 of 53 when longitudinal samples were also included (66%, 95% CI 52, 78%). During the follow-up, 14 of 45 (31%) iRBD patients converted to a synucleinopathy (nine Parkinson's disease, three dementia with Lewy bodies, one MSA, one pure autonomic failure) a mean 2.5 years (SD = 2.2 years, range = 0.2–7.9 years) after lumbar puncture. RT-QuIC positivity was found in 9 of 14 (64%, 95% CI 35, 87%) of these converters at baseline. The average T_{lag} of the reactions seeded with iRBD CSF samples was 82 h, significantly higher than in Parkinson's disease patients (66 h, $P = 0.01$; Table 2). The average T_{50} was 90 h and this was also significantly higher compared to Parkinson's disease patients (77 h, $P = 0.02$). Only two iRBD patients had a particularly high V_{max} value of $>100\,000$ RFU/h and V_{max} was significantly lower compared to Parkinson's disease patients ($P = 0.02$; Fig. 1D).

The RT-QuIC positivity was similar for iRBD cohorts (around 90%) except for the DeNoPa cohort, which was lower (39%; Table 5). There was no suggestion of any differences in the clinical parameters between the four cohorts (Table 5), except the MDS-UPDRS III being higher in the Discovery and McGill cohorts compared to the DeNoPa and Bologna cohorts ($P = 0.002$). Furthermore, the iRBD patients in the Bologna cohort were older compared to other cohorts, although this was not statistically significant. In the DeNoPa cohort, we found 7 of 18 (39%, 95% CI 17, 64%) iRBD patients positive for αSyn-RT-QuIC at any time point. In two

patients, the baseline sample was negative, but the subsequent follow-up samples were positive (Supplementary Table 6). Seven converted to synucleinopathy (four Parkinson's disease, three dementia with Lewy bodies), but the positive RT-QuIC reaction was only detected in two before conversion. In the Bologna cohort, 10 of 11 (91%, 95% CI 59, 100%) iRBD patients were positive for αSyn-RT-QuIC. Three converted to synucleinopathy (two Parkinson's disease and one MSA) and all were RT-QuIC-positive. In the Montreal cohort, 9 of 10 (90%, 95% CI 55, 100%) iRBD patients were positive for αSyn-RT-QuIC. Two converted to Parkinson's disease and both were RT-QuIC-positive. In the Discovery cohort, five of six (83%, 95% CI 36, 100%) iRBD patients were positive for αSyn-RT-QuIC. Two converted to synucleinopathy (one Parkinson's disease and one pure autonomic failure) and were RT-QuIC-positive. However, Kaplan–Meier analysis of the total iRBD cohort showed no evidence that RT-QuIC positives had a higher risk of conversion (Fig. 3).

When we looked at RT-QuIC parameters against disease severity (Supplementary Table 7), we found modest evidence that MDS-UPDRS I was associated with F_{max} ($P = 0.03$) and AUC ($P = 0.04$), and RBD duration was associated with V_{max} ($P = 0.03$), but these associations were not in the expected direction (i.e. higher V_{max} with shorter duration). When adjusted for potential confounders, the associations of MDS-UPDRS I with F_{max} and AUC remained but RBD duration with V_{max} was attenuated (Supplementary Table 8). There was also some modest evidence that increasing RBD duration was associated with F_{max} ($P = 0.03$) and that urinary dysfunction was associated with T_{lag} ($P = 0.05$) and T_{50} ($P = 0.03$), but none in the expected direction. It seems that being male gender was related to higher V_{max} ($P = 0.017$), F_{max} ($P = 0.005$) and AUC ($P = 0.008$). There was also moderate evidence that worse MMSE scores were associated with a higher V_{max} ($P = 0.03$).

Discussion

αSyn seeding aggregation assays are increasingly used in various laboratories with high sensitivity and specificity for Parkinson's disease and dementia with Lewy bodies. However, the diagnostic criteria for widespread clinical implementation of the αSyn RT-QuIC are still not well defined. Both RT-QuIC or related protein misfolding cyclic amplification (PMCA) vary drastically in terms of

Table 4 Associations between RT-QuIC parameters and clinical progression data for 23 MSA patients

Clinical data	RT-QuIC-positive odds ratios (95% CI and P-value)	T_{lag}	V_{max}	T_{50}	F_{max}	AUC
UMSARS baseline	0.70 (0.18, 2.74); P = 0.61	−0.54 (−1.11, 0.03); P = 0.063	−0.38 (−0.98, 0.22); P = 0.20	−0.60 (−1.19, −0.02); P = 0.045	−0.15 (−0.77, 0.46); P = 0.61	−0.41 (−0.97, 0.16); P = 0.14
UMSARS follow-up[b]	1.62 (0.32, 8.13); P = 0.56	−0.37 (−1.18, 0.45); P = 0.35	−0.21 (−1.04, 0.62); P = 0.60	−0.49 (−1.31, 0.34); P = 0.23	0.03 (−0.76, 0.82); P = 0.93	−0.19 (−0.96, 0.57); P = 0.60
UMSARS change[c]	NA	0.69 (0.12, 1.25); P = 0.021	0.70 (0.15, 1.26); P = 0.016	0.56 (−0.08, 1.20); P = 0.083	0.67 (0.15, 1.19); P = 0.015	0.68 (0.18, 1.18); P = 0.011
MSA subtype (MSA-C versus MSA-P)	NA	0.59 (−0.42, 1.60); P = 0.27	0.54 (−0.46, 1.54); P = 0.27	0.19 (−0.86, 1.24); P = 0.70[a]	0.74 (−0.24, 1.72); P = 0.13	0.85 (−0.10, 1.80); P = 0.077
Age at lumbar puncture	0.96 (0.37, 2.47); P = 0.93	−0.18 (−0.65, 0.30); P = 0.45	−0.19 (−0.66, 0.28); P = 0.41	0.12 (−0.38, 0.61); P = 0.63[a]	−0.18 (−0.64, 0.28); P = 0.42	0.03 (−0.42, 0.48); P = 0.89
Disease duration	1.77 (0.54, 5.80); P = 0.34	0.09 (−0.38, 0.57); P = 0.69	0.13 (−0.34, 0.60); P = 0.57	0.01 (−0.48, 0.51); P = 0.96[a]	0.11 (−0.35, 0.57); P = 0.62	0.05 (−0.40, 0.50); P = 0.81
Gender (male versus female)	1.40 (0.21, 9.49); P = 0.73	−0.21 (−1.20, 0.79); P = 0.67	0.03 (−0.96, 1.01); P = 0.96	−0.15 (−1.18, 0.89); P = 0.77[a]	−0.28 (−1.25, 0.68); P = 0.55	−0.67 (−1.60, 0.27); P = 0.15

Both exposures and outcomes standardized to unit standard deviation to aid interpretability. Adjusted for sex, MSA subtype, age and disease duration at lumbar puncture. RT-QuIC-positive response not adjusted for MSA subtype due to perfect prediction. Note that T_{lag} and T_{50} were inverted to normalize the distribution. NA = model could not be formulated due to perfect prediction.

[a]Evidence the residuals are not normally distributed.

[b]Only 20 had follow-up data.

[c]Change from baseline to follow-up divided by number of years between assessments.

the protocols used and have shown variable inter-laboratory consistencies.[29,30,49–51] Furthermore, RT-QuIC is still largely considered to deliver a binary yes/no determination of the αSyn seeding and the clinical use of various quantitative assay parameters (e.g. T_{lag}, T_{50}, V_{max}, AUC, F_{max}) have not been studied in detail so far. Here we show that αSyn-RT-QuIC identified Parkinson's disease with 89% sensitivity and 96% specificity in our longitudinal Discovery cohort. This is slightly lower but consistent with what we reported before in a smaller group size.[26] αSyn-RT-QuIC, far more sensitive compared to conventional αSyn ELISA, only detects those forms of αSyn capable of seeding further misfolding and thus reports on the actual process (i.e. permissive templating) central to disease pathogenesis. We were not able to identify any clinical basis for how Parkinson's disease patients with a negative αSyn-RT-QuIC result differed from their positive counterparts. Furthermore, no clear association between RT-QuIC quantitative parameters and Parkinson's disease clinical symptoms was identified. This is in concordance with Kang *et al.*[29] and Orru *et al.*,[49] who also showed no correlation between assay and clinical parameters, both studying 105 Parkinson's disease patients from the BioFIND cohort, but in contrast to a study by Shahnawaz *et al.*,[27] who showed T_{50} values of the PMCA assay to correlate with Hoehn and Yahr stage in 76 Parkinson's disease patients. Some of the effects we found between MDS-UPDRS I, MoCA and MMSE with T_{50} were not in the expected direction, so that more severe phenotype would have been associated with shorter T_{50} (i.e. higher seeding capacity). It could be that these are type I errors or they may represent real unexpected findings. Moreover, none of our assay parameters associated with motor progression (i.e. rate of change in the MDS-UPDRS III). However, it is important to note all of our results are exploratory in a small sample and need replicating to prove whether these represent true effects. Our negative findings could also be due to Discovery patients being moderately affected (mean MDS-UPDRS III score 27) at the time of CSF collection. To analyse whether the seeding capacity of pathogenic αSyn changes during disease progression, one should examine larger cohorts with longitudinal CSF samples representing wider spectrum of disease severity.

We also analysed the RT-QuIC assay parameters in four different Parkinson's disease clusters identified using a data-driven approach incorporating all functional measures (motor, mood, affect, cognition, constipation, olfaction, vagal autonomic) without any *a priori* hypotheses in 2545 early Parkinson's disease subjects.[37] Interestingly, the lowest proportion of RT-QuIC responders was found in cluster 2 with milder form of disease, whereas all cluster 1 patients with fast motor progression and worse non-motor symptoms showed a positive RT-QuIC response. We also showed that some RT-QuIC parameters (e.g. V_{max}) significantly differed across the clusters. Differences in the αSyn seeding activity could represent distinct 'strain profiles', which could be different not only between different synucleinopathies but also within a single disease entity. The structural heterogeneity of αSyn strains has been reported to be greater in Parkinson's disease than in MSA,[19] possibly reflecting the greater variability of disease phenotypes evident in Parkinson's disease.[37] How the 'strain profiles' vary within Parkinson's disease and how they relate to clinical clusters will need further investigation.

αSyn-RT-QuIC identified MSA with 75% sensitivity, which is slightly lower to 94% sensitivity reported by Shahnawaz *et al.*[52] in 65 MSA patients. However, both studies are in sharp contrast to other studies that have detected much lower seeding activity in MSA.[30,53] Thus, future research should aim for inter-laboratory RT-QuIC evaluation of these patients. Our data also showed that RT-QuIC parameters had some use in distinguishing MSA from Parkinson's disease CSF samples having longer T_{50} but significantly lower V_{max}, as has been shown by other studies.[27] The most

Table 5 Demographic characteristics in the iRBD cohorts

Variable\cohort	DeNoPa (n = 18)	Bologna (n = 11)	McGill (n = 10)	Oxford (n = 6)	P-value
RT-QuIC-positive response, n (%)	7 (38.9)	10 (90.9)	9 (90.0)	5 (83.3)	<0.001[***]
Sex, male, n (%)	11 (61.1)	8 (72.7)	8 (80.0)	6 (100.0)	0.32
Age at lumbar puncture	64.7 ± 7.8 (51.0–77.0)	70.7 ± 6.5 (55.0–88.0)	63.0 ± 9.5 (46.0–76.0)	64.0 ± 9.9 (51.2–74.1)	0.15
Duration of disease	5.8 ± 4.3 (0.7–12.0)	3.3 ± 1.7 (1.5–7.0)	5.2 ± 6.4 (0.2–20.0)	3.0 ± 1.1 (1.4–4.4)	0.56
MDS-UPDRS part I	11.7 ± 4.8 (4–20)	NA	10.3 ± 5.9 (4.7–18.5)[a]	9.7 ± 5.6 (2–17)	0.64
MDS-UPDRS part II	2.8 ± 3.0 (0–10)	NA	1.8 ± 1.9 (0.2–6.3)[a]	2.5 ± 3.0 (0–8)	0.85
MDS-UPDRS part III	3.8 ± 3.2 (0–10)	1.9 ± 2.2 (0–5)	7.9 ± 3.7 (3.5–14.3)[a]	7.5 ± 4.4 (0–12)	0.002[**]
MMSE	28.9 ± 0.8 (27–30)	28.3 ± 1.2 (27–30)	28.1 ± 1.3 (26–30)	28.7 ± 0.8 (28–30)	0.34
MoCA	25.7 ± 2.5 (21–29)	NA	26.1 ± 1.3 (25–28)	26.3 ± 1.9 (24–29)	0.96
Urinary dysfunction, %	11/18 (61.1)	2/10 (20.0)	2/9 (22.2)	2/6 (33.3)	0.10
Constipation, %	10/18 (55.6)	5/10 (50.0)	3/10 (30.0)	4/6 (66.7)	0.53
Hyposmia, %	13/18 (72.2)		7/10 (70.0)	4/6 (66.7)	1.00
Family history, %	1/18 (5.6)	2/11 (18.2)	2/10 (20.0)	2.6 (33.3)	0.31

Data are mean ± SD (range) unless otherwise stated. P-values evaluated with a Fisher's exact test or Kruskal–Wallis test.
[a]UPDRS converted to MDS-UPDRS.[48]
**P < 0.01; ***P < 0.005.
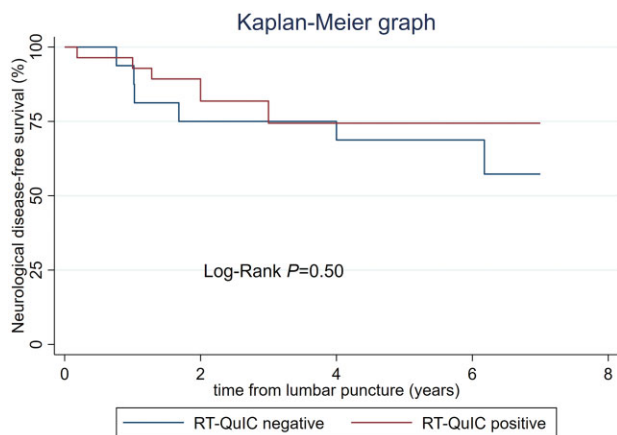
Figure 3 Kaplan–Meier analysis of iRBD patients showing rates of neurological disease-free survival according to time from baseline lumbar puncture. No evidence was seen that RT-QuIC positive iRBD patients had a higher risk of conversion than RT-QuIC negative counterparts.

likely explanation for these differences is the conformational variability of pathological αSyn species in MSA versus Parkinson's disease as has been shown by some recent studies describing biochemical (e.g. proteinase K digestion profiles) and structural (e.g. cryo-EM) differences.[19,20,52] It is important also to note that the changes in ThT kinetics do not necessarily reflect variations in seeding efficiencies as some fibrils may escape the ThT detection[54] and therefore the αSyn-RT-QuIC assay should be tested using different fluorophores, e.g. luminescent conjugated oligothiophenes.[55] Interestingly, all our RT-QuIC parameters correlated with worse clinical progression of MSA (i.e. change in UMSARS). This is a novel finding that would have great prognostic value but needs to be validated in larger cohorts; however, the fact that it is so strongly present in only 24 MSA patients is encouraging. The more severe phenotype and rapid disease progression in MSA may be one explanation why we see this relationship in MSA and not in Parkinson's disease.

Finally, for three of the four longitudinally followed iRBD cohorts we found around 90% sensitivity, identical to a recent report by Iranzo et al.[56] (90% sensitivity, 95% CI 79, 97%) and Rossi et al.[30] (100% sensitivity, 95% CI 81, 100%), but one sample (DeNoPa cohort) found a much lower sensitivity (∼40%) similar to what was recently shown by Stefani et al.[57] in olfactory mucosal samples in iRBD patients. In three cohorts, we also correctly identified all patients who had developed a synucleinopathy prior to conversion. We do not think that these cohort differences were caused by handling of the biological samples, as the CSF in each centre is collected according to stringent coherent criteria without any freeze–thaw cycles. However, the DeNoPa cohort may be diagnosing RBD earlier from the community cases than other cohorts, and motor disease and age may explain the higher specificity in other cohorts. We did not identify any direct associations between RT-QuIC quantitative parameters and prodromal symptoms such as constipation or hyposmia, but found moderate evidence that worse MMSE scores were associated with higher seeding capacity (i.e. higher V_{max}). Interestingly, also being male was related to higher seeding capacity (i.e. higher V_{max}, F_{max} and AUC). Our results highlight the importance to look for reasons for this potential cohort effect as well as further examine the natural history of iRBD patients to understand why some converters may be RT-QuIC negative. The iRBD cases should also be tested with further optimized RT-QuIC employing multiple fluorophores to capture full diversity of αSyn species.[54,55]

In summary, the significant strength of our study is to examine the relationship between quantitative RT-QuIC parameters in relation to disease progression in all three synucleinopathies: Parkinson's disease, MSA and iRBD including cohorts with very careful longitudinal clinical assessment. Our study confirmed our previous and several other studies findings about the high sensitivity and specificity of CSF αSyn-RT-QuIC for Parkinson's disease, but also showed that quantitative RT-QuIC parameters, although not correlating with clinical severity, added value alongside standard clinical data in diagnosing Parkinson's disease. Furthermore, we confirmed that CSF samples of MSA had different RT-QuIC kinetics from those of Parkinson's disease and, for the first time, showed that the RT-QuIC quantitative data seemed to correlate with disease progression of MSA. We also provided further evidence that αSyn-RT-QuIC has potential to be an early biomarker in iRBD patients. There are some caveats to our study that we cannot rule out: low number of MSA cases, lack of longitudinally collected CSF samples and examining RT-QuIC readout with ThT alone may

be considered the most notable limitations. We believe that future efforts should focus on further optimization of the assay using multiple fluorophores, improving the mechanistic insight to the determinants of αSyn aggregation that relate to assay quantification and inter-laboratory comparison of the assays. These measures are prerequisite for the widespread clinical implementation of the αSyn RT-QuIC in future.

Acknowledgements

Funding

Competing interests

The authors report no competing interests.

Supplementary material

Supplementary material is available at *Brain* online.

References

1. Postuma RB, Berg D, Stern M, et al. MDS clinical diagnostic criteria for Parkinson's disease. *Mov Disord*. 2015;30(12):1591–1601.
2. Hely MA, Reid WG, Adena MA, Halliday GM, Morris JG. The Sydney multicenter study of Parkinson's disease: The inevitability of dementia at 20 years. *Mov Disord*. 2008;23(6):837–844.
3. McKeith IG, Dickson DW, Lowe J, et al.; Consortium on DLB. Diagnosis and management of dementia with Lewy bodies: Third report of the DLB Consortium. *Neurology*. 2005;65(12):1863–1872.
4. Gilman S, Wenning GK, Low PA, et al. Second consensus statement on the diagnosis of multiple system atrophy. *Neurology*. 2008;71(9):670–676.
5. Hughes AJ, Daniel SE, Kilford L, Lees AJ. Accuracy of clinical diagnosis of idiopathic Parkinson's disease: A clinico-pathological study of 100 cases. *J Neurol Neurosurg Psychiatry*. 1992;55(3):181–184.
6. Miki Y, Foti SC, Asi YT, et al. Improving diagnostic accuracy of multiple system atrophy: A clinicopathological study. *Brain*. 2019;142(9):2813–2827.
7. Barber TR, Lawton M, Rolinski M, et al. Prodromal Parkinsonism and neurodegenerative risk stratification in REM sleep behavior disorder. *Sleep*. 2017;40(8):40.
8. Iranzo A, Tolosa E, Gelpi E, et al. Neurodegenerative disease status and post-mortem pathology in idiopathic rapid-eye-movement sleep behaviour disorder: An observational cohort study. *Lancet Neurol*. 2013;12(5):443–453.
9. Iranzo A, Fernández-Arcos A, Tolosa E, et al. Neurodegenerative disorder risk in idiopathic REM sleep behavior disorder: Study in 174 patients. *PLoS One*. 2014;9(2):e89741.
10. Schenck CH, Boeve BF, Mahowald MW. Delayed emergence of a parkinsonian disorder or dementia in 81% of older men initially diagnosed with idiopathic rapid eye movement sleep behavior disorder: A 16-year update on a previously reported series. *Sleep Med*. 2013;14(8):744–748.
11. Postuma RB, Iranzo A, Hu M, et al. Risk and predictors of dementia and parkinsonism in idiopathic REM sleep behaviour disorder: A multicentre study. *Brain*. 2019;142(3):744–759.
12. Braak H, Tredici KD, Rüb U, de Vos RAI, Jansen Steur ENH, Braak E. Staging of brain pathology related to sporadic Parkinson's disease. *Neurobiol Aging*. 2003;24(2):197–211.
13. Brettschneider J, Del Tredici K, Lee VM, Trojanowski JQ. Spreading of pathology in neurodegenerative diseases: A focus on human studies. *Nat Rev Neurosci*. 2015;16(2):109–120.
14. Jucker M, Walker LC. Self-propagation of pathogenic protein aggregates in neurodegenerative diseases. *Nature*. 2013;501(7465):45–51.
15. Bousset L, Pieri L, Ruiz-Arlandis G, et al. Structural and functional characterization of two alpha-synuclein strains. *Nat Commun*. 2013;4:2575.
16. Peng C, Gathagan RJ, Covell DJ, et al. Cellular milieu imparts distinct pathological alpha-synuclein strains in alpha-synucleinopathies. *Nature*. 2018;557(7706):558–563.
17. Peelaerts W, Bousset L, Van der Perren A, et al. alpha-Synuclein strains cause distinct synucleinopathies after local and systemic administration. *Nature*. 2015;522(7556):340–344.

18. Lau A, So RWL, Lau HHC, et al. alpha-Synuclein strains target distinct brain regions and cell types. *Nat Neurosci.* 2020;23(1): 21–31.

19. Strohaker T, Jung BC, Liou SH, et al. Structural heterogeneity of alpha-synuclein fibrils amplified from patient brain extracts. *Nat Commun.* 2019;10(1):5535.

20. Schweighauser M, Shi Y, Tarutani A, et al. Structures of α-synuclein filaments from multiple system atrophy. *Nature.* 2020; 585(7825):464–469.

21. Malek N, Swallow D, Grosset KA, Anichtchik O, Spillantini M, Grosset DG. Alpha-synuclein in peripheral tissues and body fluids as a biomarker for Parkinson's disease—A systematic review. *Acta Neurol Scand.* 2014;130(2):59–72.

22. Ruffmann C, Bengoa-Vergniory N, Poggiolini I, et al. Detection of alpha-synuclein conformational variants from gastro-intestinal biopsy tissue as a potential biomarker for Parkinson's disease. *Neuropath App Neurobiol.* 2018;44(7):722–736.

23. Ruffmann C, Parkkinen L. Gut feelings about alpha-synuclein in gastrointestinal biopsies: Biomarker in the making? *Mov Disord.* 2016;31(2):193–202.

24. Beach TG, White CL 3rd, Hladik CL, et al.; Arizona Parkinson's Disease Consortium. Olfactory bulb alpha-synucleinopathy has high specificity and sensitivity for Lewy body disorders. *Acta Neuropathol.* 2009;117(2):169–174.

25. Doppler K, Ebert S, Uceyler N, et al. Cutaneous neuropathy in Parkinson's disease: A window into brain pathology. *Acta Neuropathol.* 2014;128(1):99–109.

26. Fairfoul G, McGuire LI, Pal S, et al. Alpha-synuclein RT-QuIC in the CSF of patients with alpha-synucleinopathies. *Ann Clin Transl Neurol.* 2016;3(10):812–818.

27. Shahnawaz M, Tokuda T, Waragai M, et al. Development of a biochemical diagnosis of Parkinson disease by detection of alpha-synuclein misfolded aggregates in cerebrospinal fluid. *JAMA Neurol.* 2017;74(2):163–172.

28. Groveman BR, Orru CD, Hughson AG, et al. Rapid and ultra-sensitive quantitation of disease-associated alpha-synuclein seeds in brain and cerebrospinal fluid by alphaSyn RT-QuIC. *Acta Neuropath Comm.* 2018;6:7.

29. Kang UJ, Boehme AK, Fairfoul G, et al. Comparative study of cerebrospinal fluid alpha-synuclein seeding aggregation assays for diagnosis of Parkinson's disease. *Mov Disord.* 2019;34(4): 536–534.

30. Rossi M, Candelise N, Baiardi S, et al. Ultrasensitive RT-QuIC assay with high sensitivity and specificity for Lewy body-associated synucleinopathies. *Acta Neuropath.* 2020;140(1):49–62.

31. Chen-Plotkin AS, Albin R, Alcalay R, et al. Finding useful biomarkers for Parkinson's disease. *Sci Transl Med.* 2018;10(454): eaam6003.

32. Mollenhauer B, Trautmann E, Sixel-Döring F, et al.; DeNoPa Study Group. Nonmotor and diagnostic findings in subjects with *de novo* Parkinson disease of the DeNoPa cohort. *Neurology.* 2013;81(14):1226–1234.

33. Mollenhauer B, El-Agnaf OM, Marcus K, Trenkwalder C, Schlossmacher MG. Quantification of α-synuclein in cerebrospinal fluid as a biomarker candidate: Review of the literature and considerations for future studies. *Biomarkers Med.* 2010;4(5): 683–699.

34. Kang JH, Irwin DJ, Chen-Plotkin AS, et al.; Parkinson's Progression Markers Initiative. Association of cerebrospinal fluid beta-amyloid 1-42, T-tau, P-tau181, and alpha-synuclein levels with clinical features of drug-naive patients with early Parkinson disease. *JAMA Neurol.* 2013;70(10):1277–1287.

35. Arora S, Baig F, Lo C, et al. Smartphone motor testing to distinguish idiopathic REM sleep behavior disorder, controls, and PD. *Neurology.* 2018;91(16):e1528–e38.

36. Szewczyk-Krolikowski K, Tomlinson P, Nithi K, et al. The influence of age and gender on motor and non-motor features of early Parkinson's disease: Initial findings from the Oxford Parkinson Disease Center (OPDC) discovery cohort. *Parkinsonism Rel Disord.* 2014;20(1):99–105.

37. Lawton M, Ben-Shlomo Y, May MT, et al. Developing and validating Parkinson's disease subtypes and their motor and cognitive progression. *J Neurol Neurosurg Psychiatry.* 2018;89(12): 1279–1287.

38. Foubert-Samier A, Pavy-Le Traon A, Guillet F, et al. Disease progression and prognostic factors in multiple system atrophy: A prospective cohort study. *Neurobiol Dis.* 2020;139:104813.

39. Sixel-Döring F, Trautmann E, Mollenhauer B, Trenkwalder C. Associated factors for REM sleep behavior disorder in Parkinson disease. *Neurology.* 2011;77(11):1048–1054.

40. Sixel-Döring F, Trautmann E, Mollenhauer B, Trenkwalder C. Rapid eye movement sleep behavioral events: A new marker for neurodegeneration in early Parkinson disease? *Sleep.* 2014;37(3):431–438.

41. Schenck CH, Bundlie SR, Ettinger MG, Mahowald MW. Chronic behavioral disorders of human REM sleep: A new category of parasomnia. *Sleep.* 1986;9(2):293–308.

42. Frauscher B, Iranzo A, Gaig C, et al.; SINBAR (Sleep Innsbruck Barcelona) Group. Normative EMG values during REM sleep for the diagnosis of REM sleep behavior disorder. *Sleep.* 2012;35(6): 835–847.

43. Mollenhauer B, Zimmermann J, Sixel-Döring F, et al.; DeNoPa Study Group. Monitoring of 30 marker candidates in early Parkinson disease as progression markers. *Neurology.* 2016; 87(2):168–177.

44. Antelmi E, Donadio V, Incensi A, Plazzi G, Liguori R. Skin nerve phosphorylated α-synuclein deposits in idiopathic REM sleep behavior disorder. *Neurology.* 2017;88(22):2128–2131.

45. Postuma RB, Gagnon JF, Bertrand JA, Génier Marchand D, Montplaisir JY. Parkinson risk in idiopathic REM sleep behavior disorder: Preparing for neuroprotective trials. *Neurology.* 2015; 84(11):1104–1113.

46. Lawton M, Baig F, Toulson G, et al. Blood biomarkers with Parkinson's disease clusters and prognosis: The oxford discovery cohort. *Mov Disord.* 2020;35(2):279–287.

47. Berg D, Postuma RB, Adler CH, et al. MDS research criteria for prodromal Parkinson's disease. *Mov Disord.* 2015;30(12):1600–1611.

48. Goetz CG, Stebbins GT, Tilley BC. Calibration of unified Parkinson's disease rating scale scores to Movement Disorder Society—Unified Parkinson's Disease Rating Scale scores. *Mov Disord.* 2012;27(10):1239–1242.

49. Orru CD, Ma TC, Hughson AG, et al. A rapid a-synuclein seed assay of Parkinson's disease CSF panel shows high diagnostic accuracy. *Ann Clin Transl Neurol.* 2021;8(2):374–384.

50. Candelise N, Baiardi S, Franceschini A, Rossi M, Parchi P. Towards an improved early diagnosis of neurodegenerative diseases: The emerging role of *in vitro* conversion assays for protein amyloids. *Acta Neuropathol Comm.* 2020;8(1):117.

51. Paciotti S, Bellomo G, Gatticchi L, Parnetti L. Are we ready for detecting α-synuclein prone to aggregation in patients? The case of 'Protein-Misfolding Cyclic Amplification' and 'Real-Time Quaking-Induced Conversion' as diagnostic tools. *Front Neurol.* 2018;9:415.

52. Shahnawaz M, Mukherjee A, Pritzkow S, et al. Discriminating α-synuclein strains in Parkinson's disease and multiple system atrophy. *Nature.* 2020;578(7794):273–277.

53. van Rumund A, Green AJE, Fairfoul G, Esselink RAJ, Bloem BR, Verbeek MM. alpha-synuclein real-time quaking-induced conversion in the cerebrospinal fluid of uncertain cases of parkinsonism. *Ann Neurol.* 2019;85(5):777–781.

54. De Giorgi F, Laferrière F, Zinghirino F, et al. Novel self-replicating α-synuclein polymorphs that escape ThT monitoring can spontaneously emerge and acutely spread in neurons. *Sci Adv*. 2020;6(40):eabc4364.

55. Civitelli L, Sandin L, Nelson E, Khattak SI, Brorsson AC, Kågedal K. The luminescent oligothiophene p-FTAA converts toxic Aβ1-42 species into nontoxic amyloid fibers with altered properties. *J Biol Chem*. 2016;291(17):9233–9243.

56. Iranzo A, Fairfoul G, Ayudhaya ACN, et al. Detection of α-synuclein in CSF by RT-QuIC in patients with isolated rapid-eye-movement sleep behaviour disorder: A longitudinal observational study. *Lancet Neurol* 2021;20(3):203–212.

57. Stefani A, Iranzo A, Holzknecht E, et al.; SINBAR (Sleep Innsbruck Barcelona) group. Alpha-synuclein seeds in olfactory mucosa of patients with isolated REM sleep behaviour disorder. *Brain*. 2021;144(4):1118–1126.